Reprint From "Current Trends In Magnetism," SatyaMurthy and Madhav Rao, Eds., Indian Physics Association, Tata Inst. of Fund. Research, Bombay 400005, India. (1981)

MAGNETIC AND/OR MÖSSBAUER SPECTROSCOPIC CHARACTERIZATION OF FINE DISPERSIONS OF TRANSITION METAL CATALYSTS

Part I: Magnetic Characterization of Supermagnetic Nickel in Presence of a Ferromagnetic Component

L. N. MULAY,* R. C. EVERSON,† O. P. MAHAJAN, AND P. L. WALKER, JR.

Material Sciences and Engineering Department (136 MRL Building)
The Pennsylvania State University
University Park, Pennsylvania 16802, U.S.A.

1. Introduction

Magnetic properties of catalyst-type materials, such as metal dispersions or oxides are fascinating indeed and have attracted considerable attention during recent years. One of us (LNM) previously reported on the magnetic properties of dispersions of α-Fe_2O_3 in zeolites[1-3] and of Fe^{3+} ions in silicates[4] and in glassy carbons[5]. In addition to transition-metal oxides, the very fine dispersions of 3*d* metals such as *Fe*, *Co*, and *Ni* on various (non-magnetic) substrates (*e.g.*, SiO_2, Al_2O_3) are technologically very significant because of their widespread use as industrial catalysts for heterogeneous catalysis. Significant fractions of such dispersions display "superparamagnetic properties", which permit their characterization in terms of their particles profiles (particle shape, size, and their distribution) with respect to very small particles (< 100 Å), which otherwise elude detailed characterization by standard methods (*X*-ray line broadening, etc.). Furthermore, the magnetic technique allows an *in-situ* investigation of chemisorption. However, most of the magnetic studies so far have been on meterials containing relatively low amounts (usually below 10%) of the metal which is dispersed on substrates to yield, so to speak, ideal "single phase" supermagnetic (catalytically active) systems. Studies of this nature have been reported by Carter et al.[6] and reviewed by Selwood[7] and Whyte[8]. While such studies have undoubtedly enhanced our understanding of the mechanism chemisorption of electron

*Enquiries should be addressed to this author.

†Permanent address: Chemical Engineering Department; University of Natal, Durban, S. Africa.

donor and acceptor type molecules, very few attempts have been made t thoroughly characterize commercial catalysts containing large amounts c metal (up to 70% with multiphase components) and at temperature (: employed in actual industrial-type reactons, such as the methanation. Ther fore, it seemed desirable to select and to characterize these very types c catalysts with special reference to the following considerations.

Supported metal catalysts containing large amounts of metals hav generally different metal dispersions consisting of particles of different size and phases[9]. When such catalysts are heated at high temperatures, crystallit growth occurs via a complicated mechanism which produces a rather ur defined metal dispersion. Under these conditions, an exact determinatio of particle size distribution is very difficult. However, in the case of 3 transition metals, which are used as methanation catalysts, it is possible t delineate and to characterize such dispersions by their magnetic properties Three major types of magnetic structures, which normally coexist in supporte metals such as iron, cobalt and nickel catalysts at temperatures significantl lower than their Curie points, are discussed below.

The so-called single-domain or "superparamagnetic" structures, charac teristic of very small particles, give magnetization curves which ar adequately described by the Langevin equation [Mulay[10a], Bean et al[11]] Their changes in magnetization are described by spin rotation as in norma paramagnetics. The magnetization is strongly particle size dependent an can be used for the assessment of average particle size of an assembly. Tru superparamagnetism is characteristic of a collection of very small single domain particles in which thermal energy is dominant during the magnetiza tion process ; thus no hysteresis is observed when magnetization (σ) i plotted as a function of H/T, that is, the coercive force (H_c) and remanence (σ_r) are zero.

Secondly, we consider the single-domain anisotropic particles, which car have contributions to their magnetic energy arising from their shapes an crystal structures. These "single-domain anisotropic" particles are thermally stable in the magnetic sense[12] and are characterized by significant hysteresi during magnetization, thus giving measurable values for H_c and σ_r. Stone and Wohlfarth[13] and Néel[14] first suggested that the contributions to H_c an σ_r due to the elongated shape of single-domain anisotropic particles fa outweigh any contributions from the anisotropy of crystallite alignment within the particles.

The third type of structure, which is characteristic of the 3*d* metals in their massive or bulk state, consists of relatively large multidomain ferro-magnetic particles[12], which change over to the paramagnetic state above their Curie point. Changes in magnetization with magnetic field below the Curie

temperature are caused by domain wall motion. Their magnetization curves reveal little hysteresis with negligible contributions to H_c and σ_r, especially when no impurities and strain are present.

Kneller and Luborsky[15] have carried out an elegant theoretical analysis of the contributions of each of the above structures to the coercive force and remanence as a function of the range of particle sizes. They have further substantiated their theory with supporting data obtained for iron-cobalt alloy particles (20-300Å) dispersed in mercury. Their approach and contributions by Kittel and Galt[16] have advanced our understanding of the particle profile criteria which determine transitions from the (i) superparamagnetic to single-domain anisotropic and from (ii) the single-domain anisotropic to multi-domain particles. A schematic curve showing results of these transistions is given in Fig. 1, which is based of reference (15).

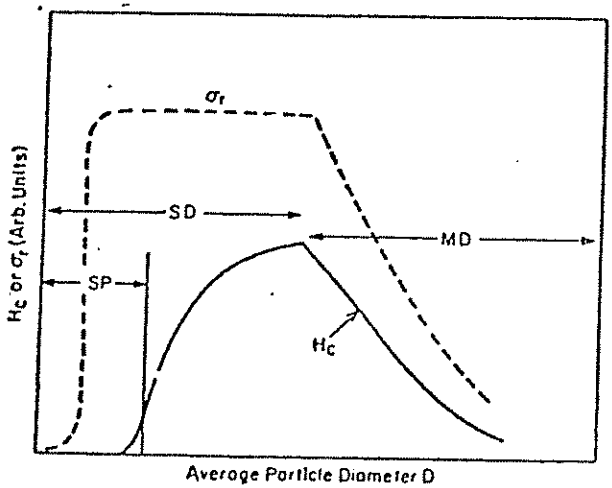

Fig. 1. Schematic representation based on reference[9] of the dependence of H_c (solid line) and σ_r (dotted line) on average particle diameter (D) for an assembly of particles consisting of the superparamagnetic (SP), single-domain anisotropic (SD) and the multidomain ferromagnetic (MD) components.

In addition to parameters such as the coercive force and remanence discussed above, information gained from magnetization (σ) versus field (H) (or versus H/T) plots is equally useful in the characterization of magnetic particles. For instance, it is possible to obtain the particle size distribution of superparamagnetic particles in the presence of the multidomain ferromagnetic component.[9] This aspect is elucidated in some detail later.

The aspects of magnetic characterization described above provide a novel approach for characterizing the growth and shape of nickel particles during the heat treatment of nickel supported on alumina. In this paper,

we present an analysis of different magnetic structures observed for two commercial samples, containing initially (sample A) 43 and (sample B) 57 wt% of total nickel, respectively, which were subjected to different heat treatments. In addition, we present particle size distribution of superparamagnetic components in the as-received and heat treated samples in the presence of multidomain ferromagnetic structures, and with special reference to this distribution around 573 K, which is quite close to the reaction temperature for methanation.

2. Experimental Methods

Apparatus :

A vibrating sample magnetometer, manufuactured by the Princeton Applied Reserach Corporation, was used for magnetic measurements. This technique was selected for the present investigation because it involved very large magnitudes of σ, σ_s and σ_r as well as H_c. The present investigation did not warrant the use of the more sensitive force-type magnetometers (available in our laboratory), which are otherwise used for the measurement of weakly dia- and para-magnetic properties. A critique of various measuring techniques including the Lewis' magnetometer is given by Mulay[10b] and the progress in magnetic instrumentation and applications relevent to this work has been appropriately reviewed biannually by Mulay and Mulay[10c] since 1962.

Magnetic fields up to KOe were generated with an electromagnet made by Varian Associates, in conjunction with 12" diam poles tapered to 6". Fields up to 20 KOe have been employed by most workers (*cf* 6-9 and references therein) at cryogenic temperatures for studies on fine particles and such were employed in the present studies ; furthermore, the special "hill climbing", computations used in the analysis of magnetization curves (described later) allowed so to speak the necessary "extrapolations" to ultra "high fields", thus obviating the need forsetting up more sophisticated equipment.

The fields were measured with a separate gaussmeter probe inserted between the poles and located very close to the vibrating sample. Magnetization measurements were recorded digitally over a wide range of magnetic fields. The magnetic field could be reversed easily to yield coercive forces as small as 10 Oe. A low temperature cryostat was used for measurements in the region 77-300°K, whereas for high temperature measurements (up to 973°K), a furnace with non inductive windings of platinum was used. This furance was surrounded by a water jacket to prevent damage to the detection coils of the magnetometer. The catalyst sample ($\sim$ 100 mg) was sealed in the lower section of a partitioned quartz tube, which in turn was attached to the lower end of a brass tube coupled to the transducer of the magneto-

meter. This arrangement permitted the sample tube to vibrate freely in the pole gap of the magnet.

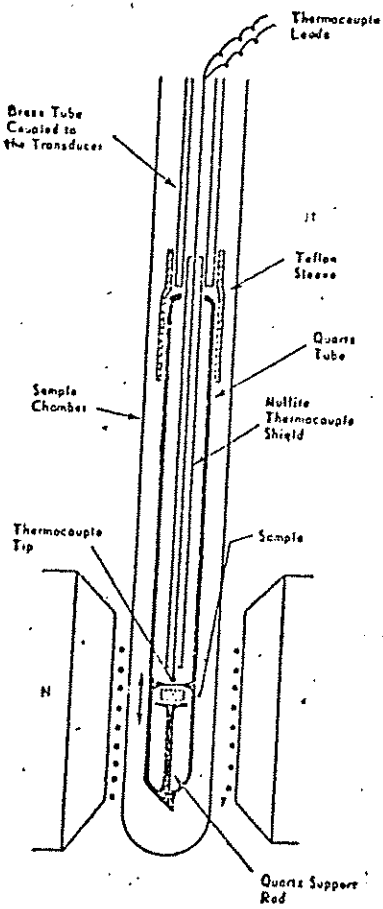

Fig. 2. Quartz tube assembly showing the sealed in position of the catalyst pellet sample. X and Y respresent the pick-up coils of the magnetometer. A platinum-wire wound furnace (not shown) slips over the quartz sample chamber to provide a uniform temperature over the catalyst sample.

The quartz tube assembly is shown in Fig. 2. It was designed so that the catalyst sample could be supported firmly in the tube. This set-up prevented unduevibration of the sample itself within the tube and consequently prevented the generation of spurious signals in the magnetometer. Furthermore, the assembly allowed the insertion of a copper-constantan thermocouple tip close to the sample for an accurate measurement of temperature. The magnetometer was calibrated with a standard spherical sample of nickel, for which the saturation magnetization (M_s) is 484 gauss, which gives the per-gram magnetization, σ_s=53.4 emu/g. [Tebble and Craik[17]]*.

*These authors and authors of papers in the J. Catalysis, etc. use "*emu/g*" or "*gauss·cm³/g*" to designate the magnetization (σ, σ_s) and the remanence (σ_r). They also use the *Oersted* (or *Gauss*) for the magnetic field (H). Conversion to S.I. units is done using the following: Magnetization of 1 Gauss=10^3 Am^{-1}; A field (H) of 1 *Oersted* (or 1 *Gauss*)=79.6 Am^{-1}. For a discussion of magnetic units see Mulay[10a], Jackson[18] and Bleaney and Bleaney[19].

The as-received and heat treated samples were reduced in H_2 and sealed under vacuum in quartz tubes prior to magnetic measurements. Reduction was for 8 hours in flowing ultrapure H_2 at 623°K followed by outgassing for 6 hours at 623°K to a final vacuum of 10^{-6} Torr. The sample was then cooled to room temperature in vacuum. Sealing of the sample tube under vacuum was carried out while the sample was surrounded by liquid nitrogen so as to p event its sintering during sealing.

3. Results and Discussion

3.1. General Characteristics of the Catalysts

Some important physical characteristics of the as-received catalysts are listed in Table I. Heat treatment of the catalysts was carried out by (a)

Table 1
Characteristics of As-Received Catalysts

Support	Catalyst $\gamma-Al_2O_3$	Catalyst $\gamma-Al_2O_3$
Nickel,* wt % (total)	43	67
Average Nickel Crystallite size, A°	185	74
BET Area, m^2/g	51	117
Pellet Size, in	1/8	3/16

*This was determined by a standard ASTM gravimetric procedure in which nickel was extracted with $HCl+HNO_3$, precipitated and weighed as a dimethyl glyoxime complex.

exposure to flowing ultrapure H_2 at 1 atm for 1 hour at selected heat treatment temperature (HTT), followed by (b) exposure to a H_2/CO synthesis mixture containing 1 mole % CO for an additional 1 hour at the HTT. The above procedures failed to cause complete reduction, which was reflected in the thermomagnetic analysis, described in a later section. This situation is not surprising in the light of reports by Martin et al.[20] who found that reduction is less than 100% complete even at 923°K.

3.2. X-Ray Diffraction Studies

Average nickel crystallite sizes for the as-received and heat treated samples were estimated from the observed X-ray line broadening for the (111) diffraction peak using the classical Debye-Scherrer equation. Strictly speaking, diffraction peak broadening is produced by a combination of crystallite size broadening, strain broadening, and defect broadening; but it is being assumed here that crystallite broading is predominant so as to be consistent with the conventional approach used in the catalysis literature. Apparently the nickel is of such small crystallite size that the (220) and (311) diffraction peaks were too weak to use for estimating crystallite size. The (200) diffraction peak was comparable in line width to the (111) peak for all heat

treatment temperatures, and thus gave similar crystallite sizes. Resul based on the broadening of the (111) diffraction peak are given in Tabl 1 and 2. It is seen that the average crystallite size for the as-receive

Table 2

Average Crystallite Size (A°) of Nickel in Heat Treated Samples.

HTT, °K	Catalyst A	Catalyst B
723	—	87
773	191	111
873	233	135
923	239	140
973	255	160

catalyst *B* is only 40% of that for catalyst *A*. This is presumably due, a least in part, to a relatively smaller loading of nickel per unit *BET* area fo catalyst *B*. For both catalysts, average crystallite size increases progressivel with increasing HTT. However, for a given HTT, the relative increase i crystallite size is more pronounced for catalyst *B* than for catalyst *A*. Fo example, the average crystallite size for catalyst *B* heat treated at 973°*K* i twice as much as that for the as-received sample, whereas the correspondin increase for catalyst *A* is only 60%.

With regard to our discussion on needle shaped particles, it should b stressed that their presence was unequivocally confirmed in catalysts *A* and *I* subjected to HTT of 773 and 923°*K* respectively by the significantly larg magnitude of H_c and σ_r (especially at low measuring temperatures); thes measurements are described later.

3.3. Thermomagnetic Analysis.

Plots of relative magnetization, $\sigma/\sigma_{s\,(bulk)}$, as a function of temperature over the range 77 to 700°*K* are shown in Fig. 3 for the as-received catalysts *A* and *B* along with the thermomagnetic curves for an "ideal" superparamagnetic dispersion of nickel[21] and for bulk nickel.[22] Unfortunately, Michel et al.[21] did not define the scale for their magnetization axis and as such no quantitative interpretation can be derived from their curve. The significance which can be attached to this curve is that the magnetization of an ideal superparamagnetic system, as expected, decreases asymptotically with temperature, because there is no magnetic interaction between the single-domain superparamagnetic particles. Furthermore, this situation, in contrast to the ferromagnetic case, prevents the possibility of any co-operative effects between domains and, consequently, forbids the onset of any phase transition, thus eliminating the appearance of a Curie temperature. For these reasons the ideal superparamagnetic behaviour is said to be analogous to the 'magnetically dilute' paramagnetic situation in which no interactions take place

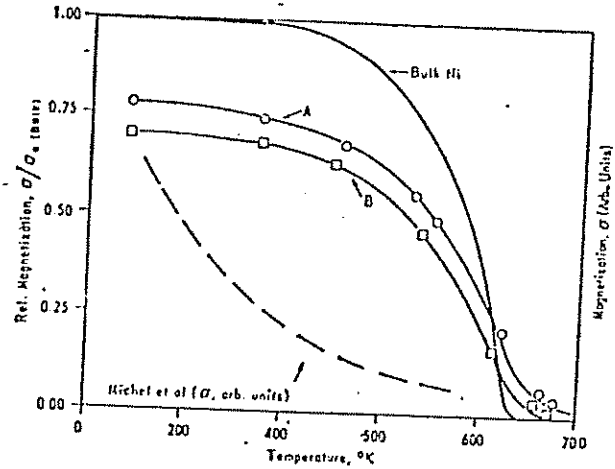

Fig. 3. Relative magnetization ($\sigma/\sigma_{s\,(bulk)}$) as a function of temperature. Here $\sigma_{s\,(bulk)}$ refers to the true saturation magnetization of bulk nickel at 0°K. The magnetization for nickel dispersions studied by Michel et al[9] is shown on the right which is in arbitrary units.

between neighbouring species[10a]. The only difference lies in the fact that a superparamagnetic particle may consist of several thousand paramagnetic species (atoms or ions). This gives rise to very large magnetic moments (of several thousand Bohr magnetons per particle) in the superparamagnetic system. In comparion to the curve of Michel et al., the curve at the top in Fig. 3 represents the characteristic ferromagnetic multidomain behaviour of bulk nickel.

Figure 3 shows that catalysts *A* and *B* have a behavior intermediate between that of bulk nickel and ideal superparamagnetic dispersion. That is, the Curie temperatures (T_C) for samples *A* and *B* are not as sharp as for bulk nickel for which $T_C = 631°K$. This fact is attributed to the presence of a substantial fraction of superparamagnetic particles in *A* and *B*. The fact that the relative magnetization, $\sigma/\sigma_{s\,(bulk)}$, for these samples does not reach the maximum value of unity can be attributed to the possibility that part of the nickel remains bound to the substrate as nickel aluminate (involving the Ni^{2+} type of paramagnetic ions), indicating incomplete reduction and equally importantly, because a large number of spins remain uncompensated on the surface of the superparamagnetic particles present in the system. Superparamagnetic particles are indeed difficult to saturate even at a field of 20 *KOe* and 70°*K*. It should be noted that these uncompensated spins and, so to speak, the holes in the *d*-band of nickel are believed to be responsible for the chemisorption of molecules and subsequent catalyzed reactions.

3.4. *Effect of Heat Treatment Temperature on H_C and σ_r.*

Figures 4 and 5 show typical plots of H_C and σ_r as a function of HTT and measuring temperature, T_m. Maxima in the plots suggest that a growth in particle size with increasing HTT has occurred. In the following paragraphs we outline some generalizations concerning both catalysts *A* and *B*, and in the last paragarph we point out differences in their magnetic behavior which characterize the changes in their particle profiles with HTT.

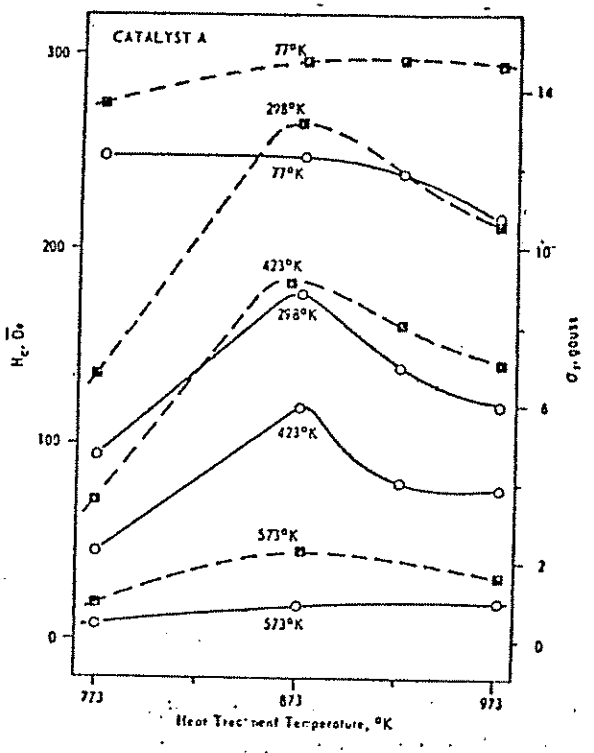

Fig 4. H_c (solid lines) and σ_r (dashed lines) as a function of heat treatment temperature for catalyst *A*. The measuring temperature is indicated on each curve.

A feature common to catalysts *A* and *B* is that over the entire range of HTT of the catalysts (773-973°*K*) the H_C and σ_r values are practically zero at $T_m = 573°K$. However, at $T_m = 423°K$ and below, significant values for H_C and σ_r are observed, which can be attributed to the formation of single-domain anisotropic (that is 'needle shaped') particles. This behavior suggests that the 'blocking temperature', T_B, for the two catayst is somewhere* between 423 and 573°*K*. This observation is consistent with Kneller and

*Extrapolation of plots of H_c versus T_m to $H_c = 0$ indicates that $T_B \sim 500°K$ for the types of systems considered here. The dependence of T_B on particle volume in the case if $Ni\text{-}SiO_2$ and $Ni\text{-}Al_2O_3$ sputtered films is discussed in detail by Gittleman and coworkers.[13]

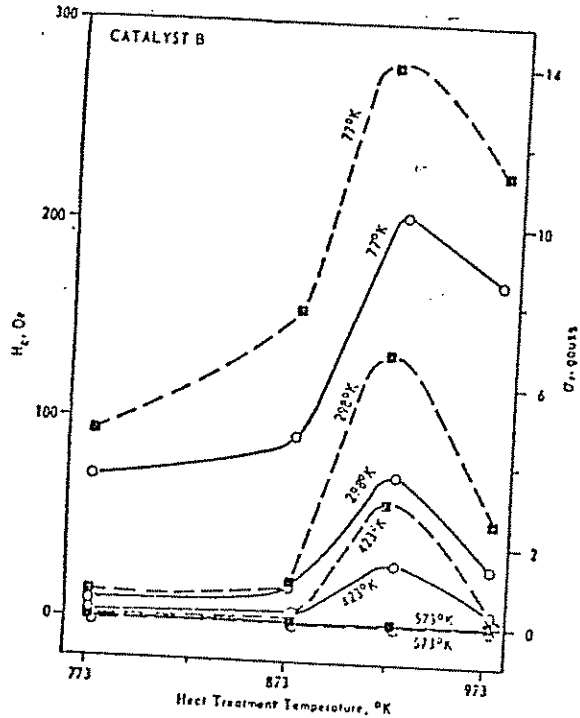

Fig. 5. H_c (Solid lines) and σ_r (dashed lines) as a function of heat treatment temperature (HTT) for catalyst *B*. The measuring temperature is indicated on each curve. Note that H_c and σ_r plots with practically zero values at a measuring temperature of 573°*K* are seen to overlap over the entire HTT range.

Luborsky's theory and their observations [15] for cobalt particles dispersed in mercury, as summarized in Fig. 1. The maxima in σ_r and H_c are attributed to the formation of single-domain anisotropic (needle shaped) particles. Furthermore, the maxima in H_c observed at specific HTT*s* suggest that these maxima result from shape anisotropies and not from crystalline anisotropies of such needle shaped particles. From published results of Kittel and Galt[16], the critical particle diameter for crystal anisotropy to become significant for nickel (*fcc*) at 300°*K* is about 438*A*° with a maximum H_c of only 135 *Oe*, whereas a maximum H_c of 3150 *Oe* can occur for needle shaped particles having a much lower diameter of about 70*A*°. Since many of the isolated particles on the catalysts have diameters much less than those required for significant crystal anisotropy as determined from hydrogen chemisorption discussed later (see ref. 24), and also because the observed coercive forces are quite large, it appears that the anisotropy contributions to H_c are mainly due to the presence of elongated (needle shaped) praticles. Electron microscopy did reveal the presence of such particles in catalysts *A* and *B* when subjected to HTT of 873 and 923°*K* respectively.

A comparison of the curves in Fig. 4 and 5 with Fig. 1 based on Kneller and Luborsky's results[15] suggests that the maxima are probably due to the following competing mechanisms (i) and (ii), which occur during the heat treatment of the catalysts :

(i) Conversion of superparamagnetic particles to single-domain anisotropic particles occurs by some migration and growth process on the catalyst surface at and below the characteristic HTT at which maximum coercivity and remanence occur.

(ii) Conversion of single-domain anisotropic particles to multidomain particles occurs via a migration and growth process above the characteristic HTT.

However, a partial conversion of superparamagnetic particles directly to multidomain particles, especially at higher temperatures, cannot be ruled out. These considerations complicate the modeling of the sintering process. Perhaps a more elaborate analysis is required than that put forward by Ruckenstein and Pulvermacher[25] and by Flynn and Wanke[26].

Catalysts *A* and *B* show maximum values of $H_C = 250$ *Oe* and 200 *Oe*, respectively, and of $\sigma_r \simeq 14$ *gauss* at $T_m = 77°K$. The fact that *A* showed the maximum in H_C at a lower HTT than *B* suggests that *B* is more resistant, in the thermal sense, to the formation of needle shaped particles and/or to their conversion to multidomain particles.

3.5. Magnetization Versus H/T Curves.

Curves for the relative magnetization σ/σ_s as a function of H/T were obtained for the as-received and heat treated nickel catalysts *A* and *B*, using fields up to 20 *KOe* and over a range of T_m, generally between 300 and 600°*K*.

Typical magnetization plots for catalyst *B* are given in Fig. 5*a*. In the dis-

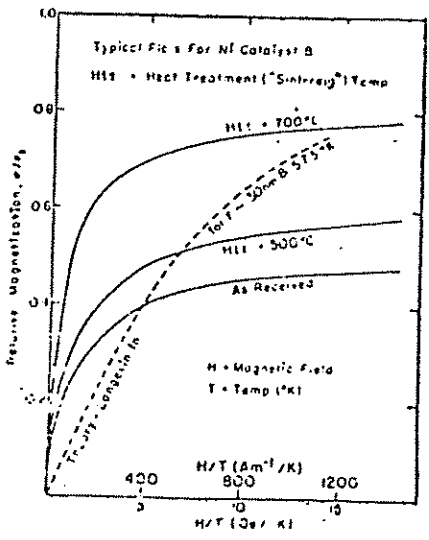

Fig. 5. (*a*) Typical magnetization (σ/σ_s)*vs* (H/T) curves for catalyst *B* for the as-received and heat treated samples. A magnetization curve for superparamagnetic particles (30 *A*° radius at 573° *K*) is shown for comparison.

cussion to follow we consider the plots obained at 573°K only (Fig. 6 and 7

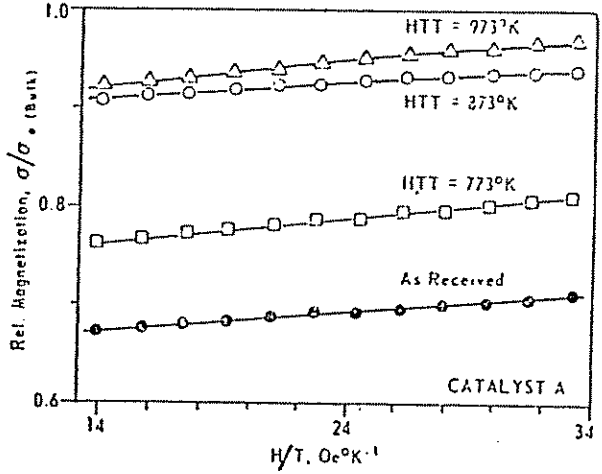

Fig. 6 Relative magnetization (σ/σ_s) plots as a function of the ratio Field (H)/Measuring Temp. (T), for catalyst A for the "high field" region. The heat treatment temperature (HTT) of each sample is indicated on the curve.

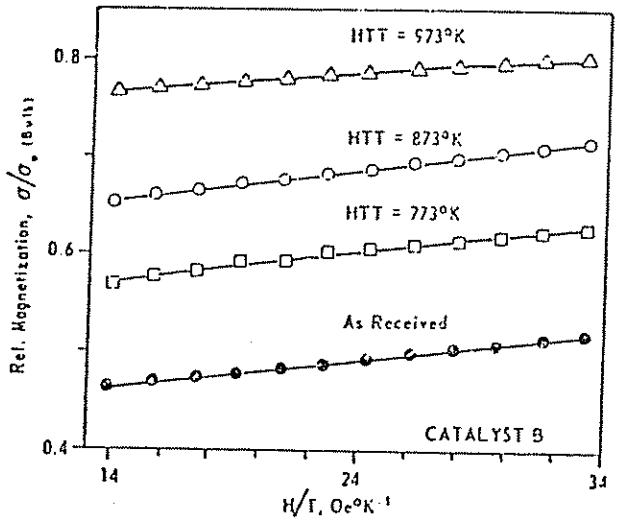

Fig. 7. Releative magnetization (σ/σ_s) as a function of the ratio Field (H)/Measuring Temp. (T), for catalyst B for the "high field" region. The heat treatmet temperature (HTT) of each sample is indicated on the curve.

for several reasons. First, this temperature is within the range of temperature over which methanation is usually conducted, and as such any quantitative interpretation derived from the magnetization curves at this temperature would be expected to have a direct technological relevance. Second, at this temperature any single-domain anisotropic particles would be expected to behave essentially as superparamagnetic particles and thus make a minor

contribution to σ_r and Hc. That is, as discussed in an earlier section concerning T_B and with reference to Figs, 4 and 5, σ_r and Hc were indeed found to be almost zero $T_m = 573°K$. In adition to these criteria we found that a temperature of $573°K$ was most suited because it was well below the Curie temperature of nickel ($631°K$) and thus yielded large values of σ which could easily be measured to the desired accuracy.

The above discussion points to the situation that at $573°K$ it is sufficient to consider the presence of only two types of particles, namely the superparamagnetic and the multidomain ferromagnetic. In analyzing the magnetization curves we have adopted a new approach in that we estimate the fraction and the mean particle volume for the superparamagnetic component in the presence of the multidomain ferromagnetic particles. It should suffice to point out that the magnetization curves for a two component systems[9,27] show a steep slope in the low field region, resembling the behavior of a ferromagnetic system ; at high fields the approach to saturation is rather slow, like that of superparamagnetic particles. Thus, at high fields the total magnetization is composed of a constant saturation magnetization component arising from the ferromagnetic fraction $(1-x_i)$ and another (variable) component which is strongly dependent on the particle size of the superparamagnetic fraction (x_i), which obeys the Langevin equation. Thus, the equation for the high field magnetization is given by

$$\frac{\sigma}{\sigma_s} = \left(1 - \sum x_i\right) + \sum_i x_i L \frac{I_{sp}\bar{v}_i H}{kT}. \qquad (1)$$

The expression under the summation sign refers to the superparamagnetic articles ; L denotes the Langevin function, $\bar{v}_i$ is the mean volume of the particles within the x_i fraction, and I_{sp} is the spontaneous magnetization for bulk nickel.[17] This equation can be be fitted by a regression routine to experimental data for the evaluation of x_i and a mean particle volume v_i as proposed by Selwood and co-workers[7,28-30]. The Langevin term[7] for particles with mean volume $\bar{v}$ is given by :

$$L = \frac{I_{sp}\bar{v}H}{kT}. \qquad (2)$$

where the product $I_{sp}\bar{v}$ represents the saturation magnetic moment of the particle. A value of $I_{sp} = 32.5$ *gauss* was taken for bulk nickel at $573°K$[17].

The high field results shown in Figs. 6 and 7 were analyzed to estimate the parameters $\Sigma \bar{x}_i$ and v_i as given by Eqs. 1 and 2. For this purpose a computer program for non-linear regression analysis of the data was used, which incorporated a hill climbing procedure. This program easily accomplished convergence, and a very good fit was obtained between the computed values (shown by a solid line in Figs. 6 and 7) and the experimental data points.

The estimates of the fractions of superparamagnetic particles, relative to the total metal present in the two catalysts, and the mean particle sizes within the superparamagnetic fractions obtained by computer analysis are shown in Table 3. The increased transformation to multidomain particles at high

Table 3.
Effect of Heat Treatment on Superparamagnetic Particles in Catalysts *A* and *B*

Heat Treatment Temperature, K	Superparamagnetic Particles			
	Wt Fraction		Mean Particle Diameter, Å	
	A	B	A	B
As received	0.36	0.58	25	24
773	0.27	0.48	39	25
873	0.21	0.40	54	28
973	0.12	0.26	37	26

HTT is evident. The transformation to multidomain particles is accompanied by a marked overall magnetic structural change characteristic of 3*d* transition metals. Changes in the mean particle size of the superparamagnetic fraction are less marked for catalyst *B*, in line with its lower loading of nickel per unit area.

It is noteworthy that the mean particle size of the superparamagnetic particles for both catalysts decreases with increase in HTT from 873 to 973°K; the decrease is more pronounced for catalyst *A*. These results suggest that during heat treatment in this temperature range, supported nickel particles undergo redispersion resulting in the formation of smaller particles. Similar observations have been reported by several workers (*cf* 30). Furthermore, Fiedorow and Wanke[31] have recently shown that when alumina supported platinum catalysts are heated in oxygen, significant changes in platinum dispersion occur over a certain HTT range.

3.6. Chemisorption of Hydrogen ;

Another distinction between the two samples was observed in terms of their hydrogen chemisorption, which was studied by standard techniques.[5] These techniques yeild the number of hydrogen atoms chemisorbed on the surface of the catalyst, which in turn corresponds to the number of surface nickel atoms.

From these results the percent degree of dispersion (f) is calculated simply as the fraction $f = (Ni$ atoms at the surface ÷ total number of nickel atoms in the bulk per gram of catalysts) × 100. Relevant information is given in Table 4, which again shows that the catalyst *B* has an overall better degree of dispersion (and hence better catalytic activity) than catalyst *A* over the entire range of HTT.

Table 4.
Results of Hydrogen Chemisorption

HTT°C	Sample *A*		Sample *B*	
	No. of *Ni* atoms per $g(x\ 10^{19})$	Dispersion f (%)	No. of *Ni* atoms per g ($x\ 10^{19}$)	Dispersion f (%)
As received	2.26	5.12	6.93	10.01
500	2.45	5.54	6.72	9.78
600	1.48	3.36	5.38	7.82
700	1.67	3.78	5.24	7.62

The degree of dispersion is plotted as a function of the weight fraction of superparemagnetic particles in Fig. 7*a* for various heat treated samples. The

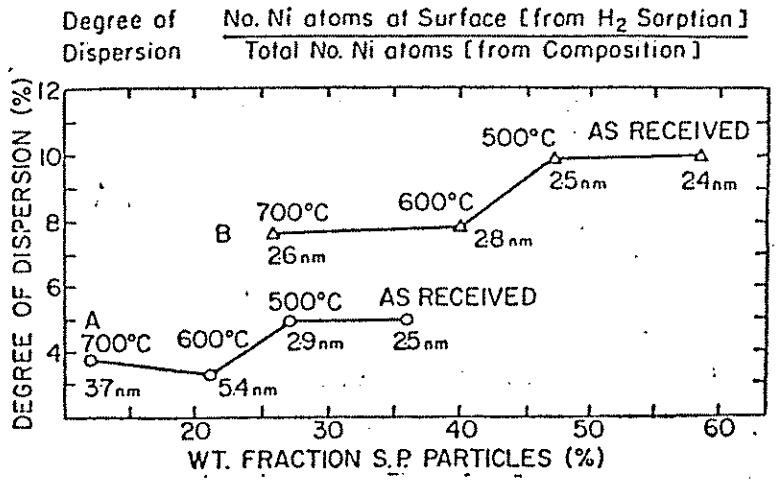

Fig. 7 (a). Plots of the degree of dispersion (f) *vs* weight fraction of superparamagnetic particles for various heat treated samples.

average particle sizes from Table 3 are also shown next to the data points for the two catalysts. This figure clearly indicates that the dispersion for *B* is indeed relatively large (7.6 to 10%), as we would expect, for smaller particles (24 to 28*A*°) with a better distribution (26 to 58%), thus this type of correlation between the results of a strictly chemisorptive technique and the magnetic technique is helpful in quantitatively characterizing the dispersions of metals such as *Ni* on diamagnetic supports.

4. Conclusions

We have shown that commercial Ni-Al_2O_3 catalysts indeed can be charcterized using magnetization (σ) versus field/termperature type measure-

ments with regard to the particle size distribution of very small catalytically active (superparamagnetic) particles in the presence of large ferromagnetic structures and under conditions close to the reaction temperature normally encountered in methanation. We have also shown that crystallite growth during heat treatment occurs from the (i) superparamagnetic to (needle) shape-anisotropic particles, and (ii) from the shape-anisotropic to very large multidomain structures These conversions also were followed remarkably well using parameters such as the coercive force and remanence. Thus, several basic concepts and theories developed in the past for the ideal single-phase systems by magneticists have been applied to the characterization of commerical catalysts of technological relevance. Our work suggests the possibility of employing magnetic characterization of quality control in the commercial production of catalysts. Further work correlating the particle profile distribution of superparamagnetic particles with their actual methanation reactivity in these commercial catalysts as well as their H_2 chemisorption ativities will be published separately.

References

[1] Mulay, L. N. and Collins, D. W., in "Amorphous Magnetism," H. Hooper and A. M. deGraff, Eds. Plenum Press, N. Y. (1973).

[2] Collins, D. W. and Mulay, L. N. (Proc. Intermag. Conf. 1968), IEEE Trans. Magnetics 4, (1993) 470.

[3] Collins, D. W., Dehn, J. T. and Mulay, L. N., in Mössbauer Methodology", Vol. III. I. J. Gruverman, Ed. Plenum Press, N. Y. (1967). (In this chapter aspects of "superparamagnetism" relevant to static magnetism and Mössbauer spectroscopy are reviewed.)

[4] Collins, D. W. and Mulay, L. N., J. Am. Ceram. Soc. 53, (1970) 74; 54, (1971) 52, 69.

[5] Mulay, L. N., Thompson, A., Walker, P. L., Jr., in "Amorphous Magnetism", H. Hooper and A. M. deGraff, Eds. Plenum Press, N. Y. (1973).

[6] Carter, J. L. and Sinfelt, J. H., J. Catal 10, (1968) 134; J. Phys Chem. 70, (1965) 3003.

[7] Selwood, P. W., "Adsorption and Collective Paramagnetism," Academic Press, N. Y., 1962; see also "Chemisorption and Paramagnetism", Academic Press, N. Y, 1975.

[8] Whyte, T. E., Jr., Catalysis Revs. 8(11), (1973) 117.

[9] Romanowski, W., Z. Anorg. Allg. Chem. 351, (1967) 180.

[10] (a) Mulay, L. N., Chapters in "Theory and Applications of Molecular Paramagnetism", L. N. Mulay and E. A. Boudreaux Eds., Wiley-Interscience, New York (1976). (This book and another with a similar title on "Molecular Diamagnetism", Wiley-Interscience, N. Y. (1976) give a succinct theoretical survey of the different types of magnetism and discuss units used in this paper).

[10] (b) Mulay, L. N., "Techniques for Measuring Magnetic Susceptibility" in "Physical Methods of Chemistry" Vol. I, Part IV, A. Weisberger and B. W. Rossiter, Eds Wiley-Interscience (1972).

[10] (c) Mulay, L. N., Analyt. Chem. 34, (1962) 343R ; Mulay, L. N. and Mulay, I. Analyt Chem. 36, (1964) 404R ; 38 ; (1966) 501R ; 40, (1968) 440R ; 42, (1970) 325 44, (1972) 324R; 46, (1974) 490R ; 48, (1976) 314R; 50, (1978) 274R ; 52, (1980) 199R
[11] Bean, C. P., and Jacobs, I. S., J. Appl. Phys. 27, (1955) 1448 ; see also Jacobs, I. and Bean, C. P., in "Magnetism" (G. T. Rado and H. Suhl, Eds.), Vol. 3, Acade Press, N. Y. 1963.
[12] Morrish, A. H., "The Physical Principles of Magnetism", Wiley, N. Y. 1965. (also Chikazumi, S "Physics of Magnetism", Wiley, N. Y. 1964).
[13] Stoner, E. C., and Wohlfarth, E. Trans. Roy. Soc. (London), A240, (1948) 599.
[14] Neel, L., Compt. rend 224, (1947) 1448.
[15] Kneller, E. F., and Luborsky, F. E., J. Appl. Phys. 34, (1963) 656 ; see also Knel E. F., "Magnetism and Metallurgy" (A. E. Berkowits and E. F. Kenller, Ed Vol. I, Academic Press, N. Y. 1969.
[16] Kittle, C., and Galt, J. K., in ' Solid State Physics" (F. Seitz and D. Turnbull, E Vol 3. p. 437, Academic Press, N. Y. (1956).
[17] Tebble, R. A., and Craik, D. J. "Magnetic Materials", Wiley, N. Y. (1969).
[18] Jackson, D. J. "Classical Electrodynamics" 5th Ed. Wiley, N. Y, (1967).
[19] Bleaney, B. I. and Bleaney, B. "Electricty and Magnetism" Oxford Univer Press, London (1965).
[20] Martin, G. A., Ceaphalen, N. deMontgolfier, P. Imelik, B. J. Chemie Phys. 70,((1973) 1422.
[21] Michel, A., Bernier, R., and LeClerc, G., J. Chem. Phys. 47, (1950) 269.
[22] Neugebauer, C. A., in "Structure and Properties of Thin Films", C. A. Neugebau Ed., Wiley, N. Y. (1959).
[23] Gittlemen, J. I., Abeles, B., and Bozowski, S., Phys. Rev. (B) 9(9), (1974) 3891 (N workers have used an AC mutual inductance bridge (10a), not requiring an exter these field for their (apparently) ideal superparamagnetic system)
[24] Everson, R. C , O. P. Mahajan, P. L. Walker, Jr. and L. N. Mulay ; J. Chem. Tec Biotechnol ; 29, (1979) 1.
[25] Ruckenstein, E., and Pulvermacher, B., J. Catalysis 29, (1973) 224.
[26] Flynn, P. C., and Wanke, S. E., J. Catalsis 34, (1974) 390.
[27] Romanowski W., Dreyer, H., and Nehring, D., A. Anorg. Allg. Chem. 310, (19 286.
[28] Abeledo, C. N., and Selwood, P. W., J. Appl. Phys 32, (1961) 2295.
[29] Dietz, R. E. and Selwood, P. W., J Appl. Phys. 3, (1961) 270.
[30] Reinen, D. and Selwood, P. W., J. Catalysis 2, (1963) 109.
[31] Fiedorow, R. M. J. and Wanke, S. E., J. Catalysis 43, (1976) 34.